

# Design of Ad Hoc Wireless Mesh Networks Formed by Unmanned Aerial Vehicles with Advanced Mechanical Automation

Ryoichi Shinkuma

Graduate School of Informatics, Kyoto University  
Yoshidahon-machi, Sakyo-ku, Kyoto, Japan, 606-8501, Japan,  
E-mail: shinkuma@i.kyoto-u.ac.jp

and

Narayan B. Mandayam

WINLAB (Wireless Information Network Laboratory), Rutgers University  
Technology Centre of New Jersey, 671 Route 1 South, North Brunswick, NJ, 08902-3390, USA

April 23, 2018

## Abstract

Ad hoc wireless mesh networks formed by unmanned aerial vehicles (UAVs) equipped with wireless transceivers (access points (APs)) are increasingly being touted as being able to provide a flexible “on-the-fly” communications infrastructure that can collect and transmit sensor data from sensors in remote, wilderness, or disaster-hit areas. Recent advances in the mechanical automation of UAVs have resulted in separable APs and replaceable batteries that can be carried by UAVs and placed at arbitrary locations in the field. These advanced mechanized UAV mesh networks pose interesting questions in terms of the design of the network architecture and the optimal UAV scheduling algorithms. This paper studies a range of network architectures that depend on the mechanized automation (AP separation and battery replacement) capabilities of UAVs and proposes heuristic UAV scheduling algorithms for each network architecture, which are benchmarked against optimal designs.

**unmanned aerial vehicle, wireless mesh network, battery replacement**

## 1 Introduction

Micro or small unmanned aerial vehicles (UAVs) have been receiving increasing attention in military, commercial, and social applications [1]. These UAVs are expected to be emerging solutions for surveying areas in which humans and ground vehicles cannot easily enter, such as untouched wilderness areas and disaster-damaged areas [2–6]. They are also operated as an ad hoc wireless mesh network infrastructure that connects such isolated areas to a communication infrastructure [7–9], which could be a promising solution, particularly for collecting sensor data obtained in these areas. The benefits of airborne relaying, in which a UAV provides an interconnection between an isolated area and a communication infrastructure, have been discussed [10]. It was reported that airborne connection provides better con-

nectivity and throughput than ground connections because three-dimensional positioning of relaying nodes provides line-of-site (LOS) propagation and suppresses shadowing and fading effects more effectively. Multihop airborne relaying and aerial wireless mesh networks that use a multi UAV system have also been proposed [7, 11]. Although those networks cover longer distances than single-hop networks, the technical problems of routing and scheduling are more complicated. Researchers have been working on routing protocols and algorithms and battery recharging scheduling for maintaining the connectivity of wireless mesh networks.

However, networks built on the basis of conventional techniques are not sufficiently effective in terms of sustainability because earlier works have not considered the following assumptions: (1) Wireless access points (APs) can be separable from UAVs and carried by UAVs. Therefore, UAVs do not need to keep flying once APs are placed at appropriate positions for connectivity. (2) UAV and AP batteries can be replaced and carried by UAVs. UAVs do not need to wait at the energy station until their batteries are fully charged. The recent development of mechanical automation for UAVs has been making these assumptions realistic. First, the automatic battery-replacement technology, which is also called battery swapping, for UAVs has been recently well-discussed [12–17]. As illustrated in Figure 1, the automatic battery-replacement technology enables UAVs to replace their discharged batteries with new ones and start flying immediately, without waiting until they are fully charged at the energy station. Moreover, the technology of load manipulation by UAVs has been developed [18–21]. With this technology, as illustrated in Figure 2, UAVs can carry small APs and batteries for the APs and place them at appropriate positions.

In this paper, we propose a new design for wireless mesh networks formed by UAVs under the assumption that both batteries and APs are replaceable and separable from UAVs and are carried and placed at the appropriate positions by the mechanical automation of UAVs. We present possible design models of UAV-formed mesh networks and discuss the advantages and disadvantages of each model. We also

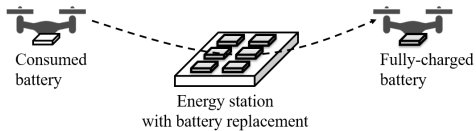


Figure 1: Automatic battery replacement

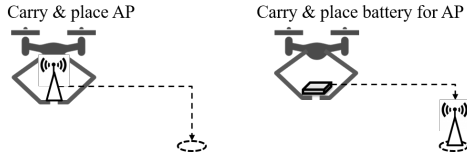


Figure 2: AP and battery carrying and placement, enabled by load manipulation

consider the number of UAVs required for maintaining the connectivity as a primary metric of how feasible the design model is and show numerical results obtained through computer simulations. In addition, we examine and present the number of required batteries and the throughput performance of our system.

Our contributions are summarized as follows: 1) we present a novel approach that addresses mesh networks formed by UAVs with replaceable batteries and separable APs; 2) we present possible design options of UAV-formed mesh networks and compare them; and 3) we study the feasibility of designing such mechanically automated networks in terms of the numbers of required UAVs and batteries and the throughput, which are evaluated by computer simulations. The differences between this paper and our previous paper [22] are summarized as follows: 1) this paper has developed the mathematical formulation of our system to discuss the baseline and the lower-bound performances in the simulation results; 2) the previous paper assumed a linear battery model without considering the non-linear characteristics of the battery; 3) the previous paper assumed an unlimited number of batteries, while this paper evaluates the required number of batteries; and 4) the throughput performance of UAV-formed mesh networks was not evaluated in the previous paper.

The remainder of this paper is organized as follows: Section 2 discusses related work. Section 3 presents the model, the problem statement, and the algorithm for UAV operation of the proposed system. Then, Section 4 demonstrates the model and presents the results of the feasibility evaluation, which uses a realistic battery model. Next, the throughput performance analysis is presented in Section 5. Finally, Section 6 concludes this paper.

## 2 Related work

This section discusses the prior works related to this paper. First, we discuss the automatic battery-replacement technology, which is one of the basic requirements of UAVs in our system. A load-manipulation technology for UAVs is assumed in our system since UAVs need to carry APs and place them at predetermined positions and carry bat-

teries for APs. Finally, we discuss prior works that have addressed scheduling problems in UAV systems.

### 2.1 Battery replacement

In 2010, Swieringa et al. demonstrated a battery swapping mechanism and online algorithms for addressing resource management, vehicle health monitoring, and precision landing onto the battery swapping mechanism’s landing platform [13].

There were many research efforts on battery replacement technology in 2011. Kemper et al. proposed three station designs for refilling platforms and one concept for battery exchange platforms [14]. They also analyzed the economic feasibility of automatic consumable replenishment stations, considered two types of stations (container refilling and container exchange), and discussed the application of these systems. They asserted that refilling platforms better suit low-coverage unmanned aerial systems (UASs), while exchange stations allow high coverage with fewer UAVs. In another work, they compared different solutions for various modules of an automated battery replacement system for UAVs [12]. They also proposed a ground station capable of swapping a UAV’s batteries and discussed prototype components and tests of some of the prototype modules. They concluded that their platform is well-suited for high-coverage requirements and is capable of handling a heterogeneous UAV fleet.

Toksoz et al. introduced a hardware platform for automated battery changing and charging for multiple UAV agents [15]. From the results of experiments in an indoor flight test facility, they concluded that their change/charge station has sufficient capability and robustness in the context of a multi-agent, persistent mission where surveillance is continuously required over a specified region. In 2015, they presented the development and hardware implementation of an autonomous battery maintenance mechatronic system that significantly extends the operational time of battery-powered small-scale UAVs [16]. This automated system quickly swaps a depleted battery of a UAV with a replenished one while simultaneously recharging several other batteries.

In 2013, Fujii et al. proposed the concept of “Endless Flyer”: they developed an automatic battery replacement mechanism that allows UAVs to fly continuously without manual battery replacement and suggested scalable and robust applications for the system. They conducted an initial experiment using this system and successfully assessed the possibility of continuous surveillance in both indoor and outdoor environments [17].

### 2.2 Load manipulation

In 2011, Pounds et al. analyzed key challenges encountered when lifting a grasped object and transitioning into laden free-flight [18]. They determined stability bounds in which the changing mass-inertia parameters of the system due to the grasped object will not destabilize the flight controller. They demonstrated grasping and retrieval of a variety of objects while hovering, without touching the ground, using the Yale Aerial Manipulator testbed.

In 2012, Palunko et al. tackled the challenging problem of using quadrotors to transport and manipulate loads safely

and efficiently. Aerial manipulation is extremely important in emergency rescue missions and in military and industrial applications [19]. They described and summarized two possible approaches that enable agile and safe load transportation using a single quadrotor UAV: 1) an adaptive controller that considers changes in the center of gravity and 2) an optimal trajectory generator based on dynamic programming for swing-free maneuvering. From the simulation results, they verified the validity of the proposed algorithms. They also presented experimental results of the proposed optimal swing-free trajectory tracking approach.

In a project named AEROWORKS, Bartelds et al. proposed a solution that combines control of the aerial manipulator’s end-effector position with an innovative design approach of aerial manipulation systems consisting of both active and passive joints [20]. The approach aimed at limiting the influence of impacts on the controlled attitude dynamics to allow the aerial manipulator to remain stable during and after impact. The experimental results showed that the proposed approach and the developed mechanical system achieve stable impact absorption without bouncing away from the interacting environment.

## 2.3 Scheduling

Cummings and Mitchell performed pioneering work on scheduling in UAV systems [23]: To study how levels of automation affect UAV knowledge-based missions and payload management control loops from a human supervisory control perspective, they conducted a simplified simulation of multiple UAVs operating independently of one another. The goal was to determine how increasing levels of automation affected operator performance to identify possible future automation strategies for multiple UAV scheduling.

In 2013, Kim et al. developed a mixed-integer linear program (MILP) model for formalizing the problem of scheduling a system of UAVs and multiple shared bases in disparate geographic locations [24]. In practice, their approach allowed for a long-term mission to receive uninterrupted UAV service by successively handing off the task to replacement UAVs served by geographically distributed shared bases.

Felice et al. investigated the utilization of low-altitude aerial mesh networks of small UAVs (SUAVs) to re-establish connectivity among isolated end-user devices located on the ground [7]. In particular, they addressed the problem of energy lifetime and proposed a distributed charging scheduling scheme through which persistent coverage of SUAV-based mesh nodes can be guaranteed in an emergency scenario. They presented a distributed algorithm that enables SUAV-based mesh nodes to autonomously decide when to recharge. Their algorithm was designed on the basis of the following requirements: (i) it attempts to preserve the connectivity index by giving precedence to SUAV-based mesh nodes whose departure will not cause the partitioning of the aerial mesh, and (ii) it accounts for the recharging need of each SUAV-based mesh node on the basis of its residual energy.

Table 1: UAV-AP models. JNT and SPT stand for joint and separate. CH and RP stand for charge and replacement.

Model	UAV-AP joint model	Battery replenishment for UAV		Battery replenishment for AP	
		Charged by ES	Battery replacement	Charged by UAV	Battery replacement
JNT-CH	✓	✓			
JNT-RP	✓		✓		
SPT-CH		✓		✓	
SPT-RP			✓		✓

## 3 Proposed System

### 3.1 UAV-AP models

We consider multiple representative classes of UAV-AP models, as summarized in Table 1. The first classification divides the models into UAV-AP joint (JNT) models and UAV-AP separate (SPT) models. In the former, UAVs work as APs when they stay at the predetermined AP positions. In the latter, UAVs and APs work separately as UAVs and APs. Furthermore, as shown in Table 1, the second classification is based on the battery replenishment strategies and classifies the models into charging (CH) and replacement (RP) models. Thus, the UAV-AP models are JNT-CH, JNT-RP, SPT-CH, and SPT-RP.

### 3.2 UAV-AP joint case

#### 3.2.1 System model

The proposed system in the UAV-AP joint case is illustrated in Figure 3. The basic components of the system are a base station (BS), UAVs, and sensor devices. As illustrated in Figure 3, some of the UAVs work as APs at the predetermined AP positions. The BS is connected to the internet and forwards sensor data to users over the internet, while the UAVs at the AP positions form a wireless mesh network for collecting sensor data from sensor devices and forward the data to the BS in a multihop manner. The BS is operated with an energy infrastructure, while the UAVs are operated with batteries. Although sensor devices are also operated with batteries, this paper does not discuss energy issues for sensor devices because, in general, their lifetimes are sufficiently long, even with small batteries [25].

JNT-CH and JNT-RP in Table 1 follow the UAV-AP joint model, in which UAVs work as APs when they stay at the AP positions. UAVs not working as APs are necessary for sustaining the lifetime of the network. When a UAV with a longer battery lifetime arrives at a predetermined position, the UAV working as an AP at that position is replaced with that one. The difference between the JNT-CH and JNT-RP models is that, while UAVs need to wait at the ES until their batteries are fully charged in JNT-CH, they can replace their batteries with well-charged ones in advance at the ES in JNT-RP. In comparison with the UAV-AP separate models, the UAV-AP joint models have advantages due to their simplicity: UAVs require no mechanisms for charging or replacing AP batteries and do not need to carry APs. This also enables us to use a simple scheduling algorithm for UAVs.

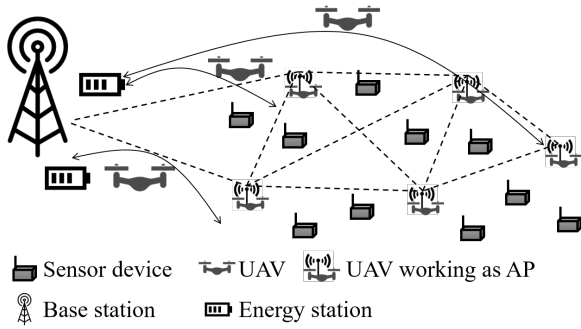


Figure 3: System model in the UAV-AP joint case

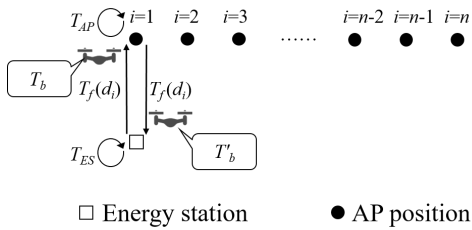


Figure 4: Model for the problem formulation

A realistic application of our system model in Figure 3 is research and prevention of disasters in untouched wilderness areas and disaster-damaged areas, where it is often difficult but important to collect sensor data. An example of such an application is detection of forest fires [26]. By collecting sensor data related to vegetation in real time, we can quickly detect when a forest fire might occur; the collected data are used to estimate the hydric stress and risk index, which enables early detection of forest fires.

### 3.2.2 Problem formulation

In the previous section, we presented a system model in the UAV-AP joint case and described the details of the two UAV-AP joint models in Table 1. In general, as the number of UAVs operated in the system increases, it becomes increasingly challenging to schedule them, place APs, place ESs, and manage the interactions among these aspects. In the rest of the paper, we work under the assumption that the smaller the number of UAVs needed to achieve specified system level performance goals is, the more desirable the configuration.

To simplify the problem formulation, in this paper, we assume that UAVs fly from an AP position to the closest ES or from an ES to an AP position; i.e., they do not directly fly between AP positions. Suppose that  $i$  and  $N$ , which are shown in Figure 4, represent the identification number and the number of AP positions and that  $d_i$  denotes the distance from AP position  $i$  to the closest ES.  $T_{ES}$ ,  $T_{AP}$ ,  $T_f$ ,  $T_b$ , and  $T'_b$  denote the required time duration for charging or replacing the battery at the ES, the battery lifetime of the AP, the one-way trip time between the ES and the AP position, the remaining battery lifetime of the UAV from the ES to the AP position, and the remaining battery lifetime of the UAV from the AP position to the

ES, respectively. The problem of minimizing the number of UAVs can be stated as

$$\min_{\rho} M(D), \quad (1)$$

where  $M$  denotes the total number of UAVs required for maintaining the sustainability of the network in the model,  $D$  is the set of distances between each AP and the closest ES, and  $\rho$  is the scheduling rule for UAVs. Every UAV in the system is autonomously operated according to  $\rho$  in a distributed manner. When UAVs are operated, three constraints must be satisfied:

$$2T_f(d_i) + T_{ES} < T_{AP} \quad (\forall i) \quad (2)$$

$$T_f(d_i) < T_b \quad (\forall i) \quad (3)$$

$$T_f(d_i) < T'_b \quad (\forall i), \quad (4)$$

where constraint (2) means that the AP lifetime must be longer than the sum of the roundtrip flying time of the UAV between the ES and the AP position and the battery charging or replacement time for every AP position. Otherwise, the network could not be sustained due to the depletion of the battery of one or more APs. Constraint (3) means that the UAV should not suffer complete battery discharge while flying to the AP position.  $T_b$  is the remaining battery lifetime after the battery has been charged or replaced at the ES. Constraint (4) means that the UAV should not suffer complete battery discharge while flying back to the ES.  $T'_b$  in the UAV-AP joint model is the remaining battery lifetime after the battery has been consumed by a UAV that worked as an AP.

In the joint AP model, at least one UAV must work as an AP at each predetermined AP position. Therefore,  $M$  should be equal to  $N + m$ , where  $N$  is the number of AP positions and  $m$  is the number of redundant UAVs not working as APs. In a basic operation in this model, the number of redundant UAVs is one for each AP position; therefore, the baseline required number of UAVs in this model is  $2N$ . The minimum number of required UAVs is  $N + 1$ , which means that only one redundant UAV is operated to maintain a network that consists of  $N$  AP positions. Consider the worst case, in which all the APs start operating and consuming their batteries simultaneously. If only one redundant UAV is used to maintain all the AP positions, constraint (2) is changed to

$$n(2T_f(d_i) + T_{ES}) < T_{AP} \quad (\forall i), \quad (5)$$

which becomes more difficult to satisfy as  $N$  increases.

Now, we compare the two UAV-AP joint models in Table 1. JNT-CH simply follows constraints (2) to (4) and (5). In the rest of the paper, we assume that the time consumed for battery replacement is negligible because it was reported that it took only approximately ten seconds in a prototyped system [15] and will be shorter in a commercialized version. Therefore, in JNT-RP,  $T_{ES}$  is zero in constraints (2) and (5). JNT-RP can satisfy constraint (5) and achieve the minimum number of required UAVs, namely,  $N+1$ , more easily than JNT-CH, which will be examined later through simulation evaluation.

### 3.2.3 Heuristic scheduling algorithm

Finding the optimal scheduling rule of UAVs directly from the optimization problem (1) is intractable because the bat-

tery discharging and charging functions are time-varying and nonlinear [27]. Therefore, we focus on heuristic algorithms – one for JNT-CH and one for JNT-RP. Every UAV in the system is autonomously operated with these algorithms in a distributed manner. The algorithms are used mainly to determine how UAVs are associated with AP positions and when UAVs fly back to the ES. Note that we assume that the information sharing necessary for scheduling UAVs in the system is ideally performed under the supervision of the BS or ES.

Figure 5 shows the flowchart for the scheduling algorithm of UAVs for JNT-CH. The notations used in the figure are defined in Table 2. In the initial state, which is denoted as a-1, the operated UAV is associated with one of the predetermined AP positions, and the initial position of the operated UAV is the associated AP position. The next step, which is denoted as a-2, judges whether another UAV  $v$  has arrived at the associated AP position after the operated UAV has arrived. If so, the operated UAV leaves for and arrives at the ES, as shown in a-3. In a-4 and a-5, the operated UAV is charged at the ES until its battery becomes full. The next step, namely, a-6, determines the AP position with which the operated UAV should be associated.  $J$  is the set of AP positions with which the number of associated UAVs is the smallest.  $K$  is the set of AP positions in  $J$  at which the remaining battery capacity is the smallest. In Figure 5,  $i_u = i_k$  ( $k \in K$ ) means that the operated UAV is associated with one of the AP positions in  $K$ . After determining the associated AP position, the operated UAV leaves for and arrives at that position.  $T_u(i_u)$  is updated to be used in a-2. Every UAV independently repeats these steps until it receives a termination instruction. The scheduling algorithm for JNT-RP is similar to the algorithm for JNT-CH described above because both follow the UAV-AP joint model, although JNT-RP adopts battery replacement. The difference between the algorithms for JNT-RP and JNT-CH is that a-4 is replaced with  $B_u(t) = B_{max}(t)$  in the algorithm for JNT-RP, which means that UAV  $u$  replaces its battery with the most-charged one at the ES, and a-5 is removed.

### 3.3 UAV-AP separate case

#### 3.3.1 System model

The proposed system in the UAV-AP separate case is illustrated in Figure 6. The basic components of the system are the same as those in the joint case (Figure 3). In the separate case, UAVs carry and place separate APs at the predetermined AP positions in advance. After that, UAVs are operated only to maintain the sustainability of the network of pre-allocated APs.

SPT-CH and SPT-RP in Table 1 follow the UAV-AP separate model, in which APs are initially placed at the predetermined positions and UAVs work to maintain AP and UAV batteries. In SPT-CH, UAVs charge their batteries at the ES, as in JNT-CH, and provide the energy capacity for APs from their batteries. In SPT-RP, UAVs are allowed to replace their batteries with well-charged batteries in advance at the ES and swap batteries with APs to sustain the lifetimes of APs. Therefore, in SPT-RP, UAVs need to be equipped with a function that enables them to swap

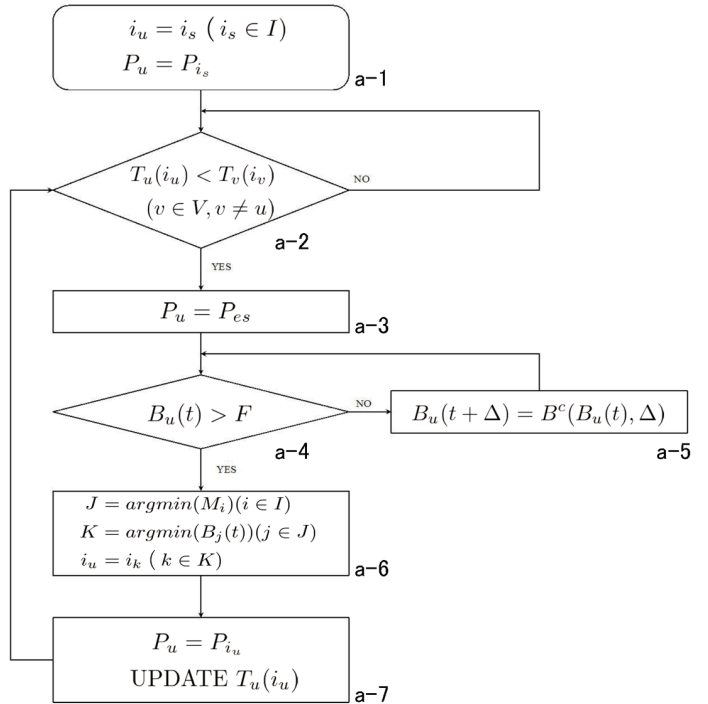


Figure 5: Flowchart of the scheduling algorithm for JNT-CH

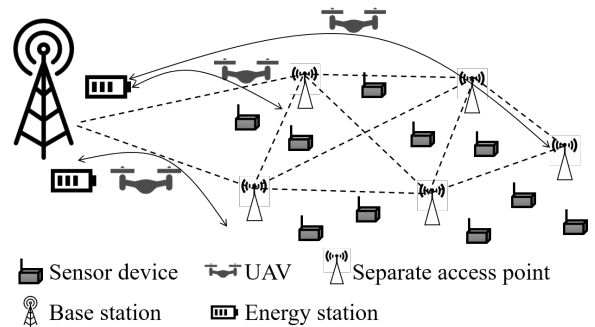


Figure 6: System model in the UAV-AP separate case

batteries with APs. In comparison with the UAV-AP joint model, the UAV-AP separate model benefits from a reduced number of required UAVs; once separate APs are placed at the predetermined positions, only the UAVs necessary for maintaining AP batteries are required.

#### 3.3.2 Problem formulation

The optimization problem and the constraints in the UAV-AP separate case can be represented by (1) and (2) to (4), respectively, as in the UAV-AP joint case. However, in the UAV-AP separate model, since separate APs are allocated to the AP positions in advance,  $M$  is equal to  $m$ . Moreover, in the UAV-AP separate model,  $T'_b$  in constraint (4) is the remaining battery lifetime after the battery has been consumed by the AP. The baseline required number of UAVs is  $N$ ;  $N$  UAVs are operated to maintain the batteries of  $N$  separate APs. Moreover, the minimum number of required UAVs is 1; only one UAV is used to maintain the sustainability of the network. Constraint (5) is applicable

Table 2: Notations in flowcharts

Parameter	Value
$i = 0, 1, 2, \dots$	AP position number
$I$	Set of $i$
$P_i = (X_i, Y_i, Z_i)$	Position of $i$
$M_i$	Number of UAVs associated with $i$
$B_i(t)$	Remaining battery capacity of device (AP or UAV) located at $i$ at time $t$
$T_v(i)$	Latest time when UAV $v$ arrived at $i$
$u$	Operated UAV
$V$	Set of UAVs
$i_u$	$i$ associated with $u$
$P_u = (X_u, Y_u, Z_u)$	Position of $u$
$B_u(t)$	Remaining battery capacity of $u$ at time $t$
$B^c(B(t), \Delta)$	Function of charging. Return $B(t)$ plus charging amount for $\Delta$ time
$B^d(B(t), \Delta)$	Function of discharging. Return $B(t)$ minus discharging amount for $\Delta$ time
$F$	Full battery capacity
$P_{es} = (X_{es}, Y_{es}, Z_{es})$	Position of ES

as the constraint for both the UAV-AP separate case and the UAV-AP joint case.

We compare the two UAV-AP separate models in Table 1. In SPT-CH, an additional term, namely,  $T_{UA}$ , should be added to constraints (2) and (5);  $T_{UA}$  is the time required to complete the battery charge from the UAV to the AP. Since we assume that the time required for battery replacement is negligible, in SPT-RP,  $T_{ES}$  is zero in constraints (2) and (5). Therefore, SPT-RP can satisfy constraint (5) and achieve the minimum number of required UAVs, which is 1, more easily than SPT-CH. This will be examined later thorough simulation evaluation.

### 3.3.3 Heuristic scheduling algorithm

Figure 7 shows a flowchart of SPT-CH, which is the UAV-AP separate and battery-charged model. The notations listed in Table 2 are also used here. The initial state, which is denoted as b-1, is the same as a-1. The next step, which is denoted as b-2, judges whether the remaining battery capacity of the associated AP is larger than that of the operated UAV. If not so, the operated UAV charges the associated AP in b-3. Although the other steps in SPT-CH are almost the same as those in JNT-CH, UPDATE  $T_u(i_u)$  is not required because APs are separated from UAVs in SPT-CH. In the flowchart of SPT-RP, which is the UAV-AP separate and battery-replacement model, b-2 is replaced with  $B_{i_u}(t) = B_u(t)$ ,  $B_u(t) = B_{i_u}(t)$ , and b-3 is removed. In addition, b-5 is replaced with  $B_u(t) = B_{max}(t)$  and b-6 is removed in SPT-RP.

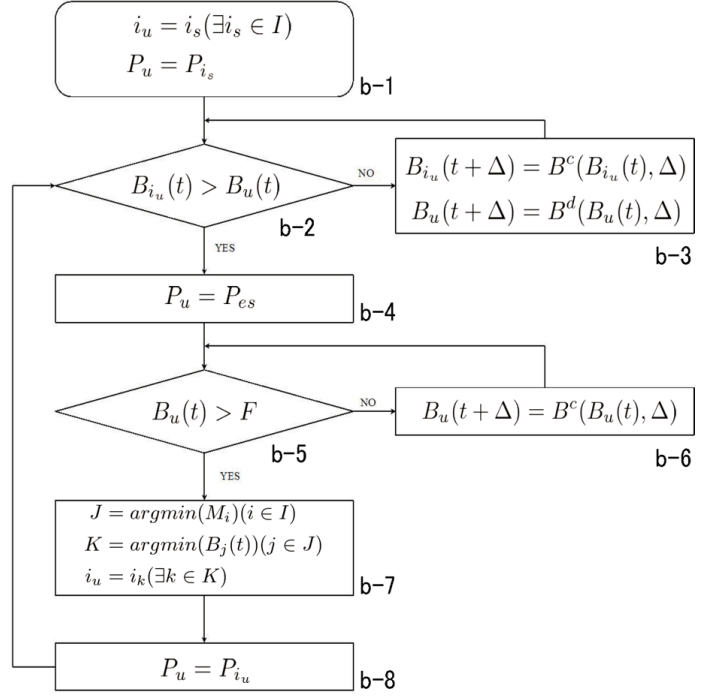


Figure 7: Flowchart of the scheduling algorithm for SPT-CH

## 4 Feasibility evaluation

This section presents and discusses the simulation model for evaluating the feasibility of the proposed system and the results. We used the number of UAVs required to maintain the system, which was the objective in the problem formulation in the previous section, as the metric for the evaluation. According to the problem formulation in the previous section, the required number of UAVs depends on the AP positions, the ES position, and the scheduling rule; it does not depend on the locations and the traffic characteristics of sensor devices, which will be considered in the throughput evaluation in Section 5. We examine the models listed in Table 1 and discussed in the previous section: JNT-CH, JNT-RP, SPT-CH, and SPT-RP. UAVs are operated in accordance with the scheduling algorithms for each model, which are described in Sections 3.2.3 and 3.3.3.

### 4.1 Simulation model

In our simulations, we used the two types of mesh topologies illustrated in Figure 8. In topology I, the AP positions are placed in alignment at intervals of 100 m. The number of AP positions  $N$  is equal to  $n$ . In topology II, the AP positions are placed in a grid, where the intervals of both row and column placements are 100 m. Therefore, in topology II, the number of AP positions  $N$  is equal to  $n^2$ . Table 3 summarizes the parameters used in our simulations, which we set not far from the specifications of recently commercialized UAVs [28]. We assumed that the separate APs and UAVs working as APs in the joint model consume a constant amount of energy for communicating. As we mentioned, we assumed that the time consumption for battery replacement is negligible. Our simulator was developed using C++.

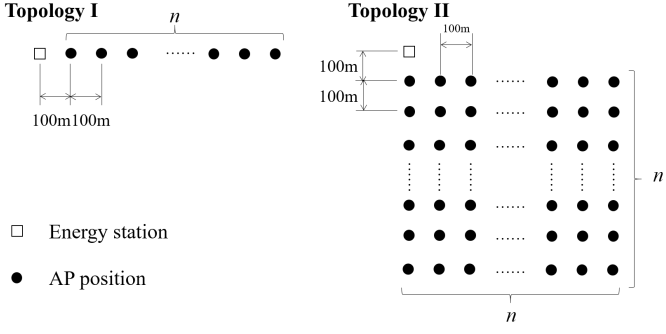


Figure 8: Simulation model for the feasibility evaluation

Table 3: Simulation parameters for the feasibility evaluation

Parameter	Value
Battery capacity	2700[mAh]
Battery power consumption when flying	18[W]
Battery power consumption when commun.	2[W]
Flying speed of UAV	15[m/s]
Battery charging efficiency from UAV to AP	100[%]
Number of charging ports of ES	Infinite

## 4.2 Battery model

Given that battery discharge models applicable to our simulations are not available yet, we developed one, which is described next. Specifically, we developed a numerical model that enables us to reproduce the nonlinear discharge characteristics of realistic batteries. The proposed discharge model is defined as a function denoted as  $discharge(X_i, P, t_s)$ , where  $X_i$ ,  $P$ , and  $t_s$  are the initial state-of-charge (SOC) value in %, the constant discharge power, and the discharge duration, respectively. The output of  $discharge(X_i, P, t_s)$  is the SOC value of the battery that has been discharged with  $P$  for  $t_s$  after the initial state. Traub reported that, although  $D - V$  (discharge capacity - voltage) curves are different for different current values  $I$ ,  $D - VI^n$  forms a unique curve upon selection of an appropriate value of  $n$ , regardless of current  $I$  [27]. We assumed the use of a lithium-ion battery (Panasonic UPF614496; 2700 mAh capacity) and used the real measurement result of the  $D - V$  curve given in [29]. For  $n = 0.081$  (which is determined using the least-squares method), the  $D - VI^n$  curve can be approximated by

$$VI^n = 3.623 \times 10^{-6} D^2 - 2.191D + 3.643 \quad (0 \leq D < 200), \quad (6)$$

$$VI^n = \frac{3.614 - 0.325D + 1.114 \times 10^{-4}}{1 - 0.094D + 1.97 \times 10^{-5} + 3.964 \times 10^{-9}} \quad (200 \leq D) \quad (7)$$

By equations (6) and (7), we can calculate the remaining capacity of a battery at any time, even after the battery has been consumed at different power levels for different purposes, i.e., flying and communicating. In Figure 9, the characteristics of the discharged battery in the cases of flying and communicating are plotted.

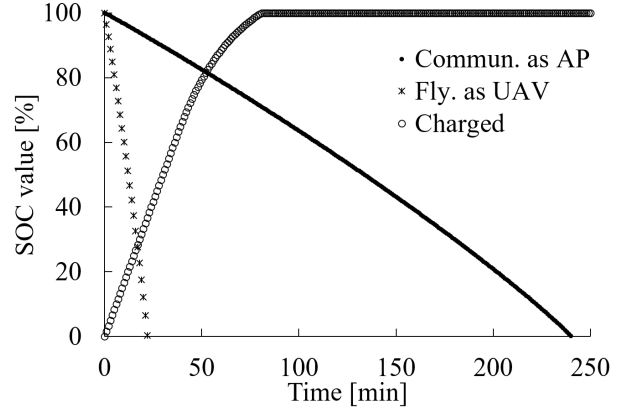


Figure 9: Charge and discharge characteristics of the battery model

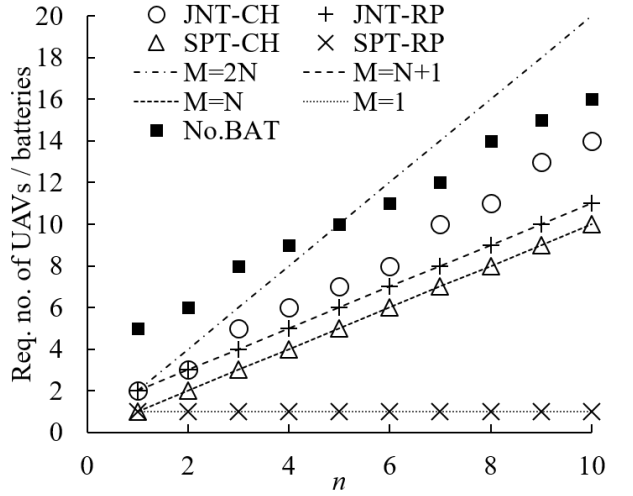


Figure 10: Numbers of required UAVs and batteries in topology I

We also developed a numerical battery charge model, which enables us to reproduce the nonlinear charge characteristic of realistic batteries. The proposed model is represented as a function denoted as  $charge(X_i, t_{ref})$ , where  $X_i$  (in %) and  $t_{ref}$  (in seconds) are the SOC value and charge duration, respectively. The output of  $charge(X_i, t_{ref})$  is the SOC value of a battery that has been charged for  $t_{ref}$  after the initial state. For validating the numerical model, we used the real  $t - C$  (time - charge capacity) curve of the lithium-ion battery given in [29]. If the battery is charged using the constant-voltage/constant-current method, the  $t - C$  curve can be approximated by

$$C = \frac{2700}{3600} t \quad (0 < t < 2238), \quad (8)$$

$$C = \frac{2700}{3600} \times 2238 + \frac{2690}{60} \frac{1}{0.0336} \{1 - \exp(-0.0336 \times 60t)\} \quad (2238 \leq t) \quad (9)$$

From these equations, we obtain the remaining capacity of a battery that has been charged for a specified amount of time after the initial state of SOC. In Figure 9, the characteristic curve of the charged battery is plotted.



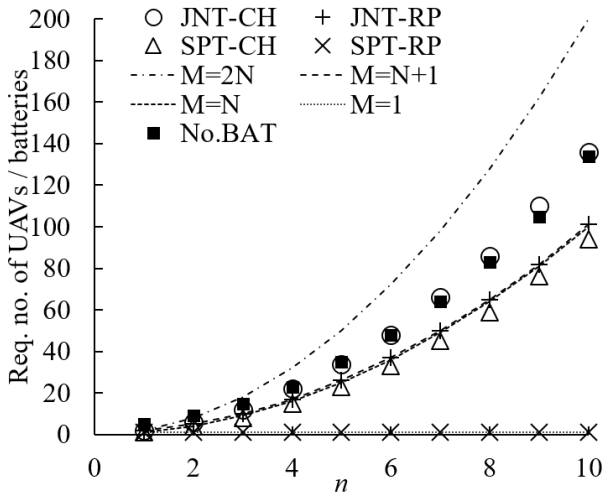


Figure 11: Numbers of required UAVs and batteries in topology II

### 4.3 Results

Figure 10 plots the number of required UAVs in the four models, namely, JNT-CH, JNT-RP, SPT-CH, and SPT-RP, for topology I. The horizontal axis corresponds to  $n$  in Figure 8. First, let us observe the results for the two UAV-AP joint models: JNT-CH and JNT-RP. As we explained in Sections 3.2.2 and 3.3.2, the theoretical baseline and lower bound for these models are  $M = 2N$  and  $M = N + 1$ , respectively. Compared with these two theoretical benchmarks, JNT-CH requires a smaller number of UAVs than the baseline, while JNT-RP achieves the lower bound. As we discussed in the previous section, since  $T_{ES}$  in JNT-RP is zero, it can easily satisfy constraint (5), which is why the number of required UAVs is reduced to the lower bound. On the other hand, to satisfy the requirement given by constraint (2), JNT-CH needs a specific number of UAVs between the baseline and the lower bound. Next, we consider the results of the two UAV-AP separate models: SPT-CH and SPT-RP. The baseline and the theoretical lower bound for the UAV-AP separate models are  $M = N$  and  $M = 1$ , respectively. As shown in Figure 10, the number of required UAVs in SPT-CH is almost the same as in the baseline, which means that SPT-CH did not work efficiently. This is because, as we mentioned in Section 3.3.2, SPT-CH incurs additional overhead because of the charging time from UAVs to APs, namely,  $T_{UA}$ , which is not included in SPT-RP. In contrast, SPT-RP achieves the lower bound. Finally, we discuss the number of required batteries in JNT-RP and SPT-RP, which is also plotted in Figure 10. It was surprising that the number of required batteries was the same for both. When a new UAV arrives at an AP position, in JNT-RP, the UAV working as an AP at that position leaves for the ES, carrying its discharged battery. In contrast, in SPT-RP, separate APs are preallocated at the positions, and the discharged batteries are carried by UAVs, which is essentially the same as in JNT-RP. In both JNT-RP and SPT-RP, at least,  $n$  batteries are necessary for  $n$  AP positions. Therefore, if we subtract  $n$  from the number of required batteries plotted in Figure 10, we observe that only 3 to 5 additional batteries are required.

Figure 11 plots the results for topology II. The trends are almost the same as those shown in Figure 10: 1) the required numbers of UAVs in both the UAV-AP joint and separate models were between the lower bound and the baseline for each model; 2) JNT-RP and SPT-RP achieved the lower bounds; and 3) SPT-CH did not reduce the number of required UAVs compared with the baseline because of its battery charging overhead from UAVs to APs. However, unlike in Figure 10, quadric-like increases in the numbers of required UAVs and batteries vs.  $n$  are shown in Figure 11. This is because the number of AP positions  $N$  increases proportionally with  $n^2$ . The additional number of batteries required in JNT-RP and SPT-RP in topology II ranged from 3 to 33, which is much larger than in the case of topology I because the number of AP positions is much larger.

In summary, JNT-RP and SPT-RP require only the lower-bound number of UAVs. They can be operated with only 3 to 5 additional batteries in topology I, while 3 to 33 additional batteries are necessary to sustain topology II. However, as we mentioned in Section 3.3.1, a technical difficulty is encountered in SPT-RP: UAVs need to be equipped with a function that enables them to swap batteries with APs, which is not necessary in the other three models. Therefore, we conclude that JNT-RP is the best option.

## 5 Throughput evaluation

### 5.1 Simulation model

In the previous sections, we used the number of required UAVs and the number of required batteries as metrics to examine the feasibility of our system. In this section, using throughput as the metric, we discuss how our system works as a wireless mesh network that delivers sensing data. We used QualNet, which is a well-known off-the-shelf software for wireless network simulations [30], to measure throughput. We assumed a scenario in which distributed sensor devices upload their sensor data to a BS located at the same position as the ES in Figure 8 via the nearest AP to each sensor device. However, we only observed throughputs of aggregated data from each AP to the BS, which we thought was sufficient for evaluating the capability of the network in collecting sensor data because we can assume that transmissions from sensor devices to APs do not affect the aggregated throughputs if the frequency channel assigned to the sensor-AP transmission is isolated from AP-AP and AP-BS transmissions. We measured the average throughput from each AP to the BS and the total throughput to determine an appropriate range of  $n$  in topologies I and II in terms of the capability of collecting sensor data.

The simulation parameters are listed in Table 4. We adopted IEEE802.11g as the wireless interface for AP-AP and AP-BS transmissions because its transmission rate is determined on the basis of the channel model more simply than more recent specifications such as 11n and 11ac [31], which use the multiple-input and multiple-output (MIMO) technology [32]. The ad hoc mode of IEEE802.11g is used for AP-AP and AP-BS links.

As the network-level setting, the ad hoc on-demand dis-



tance vector (AODV) [33] is used as the routing protocol in the wireless mesh networks. AODV is a reactive routing protocol; it does not maintain routing tables continuously but produces them only when data must be forwarded, which we believe is suitable for our system because the topology and nodes of the network can dynamically change.

As the application-level setting, to simulate traffic flows of aggregated sensor data from APs to the BS, constant-bitrate (CBR) traffic was generated at each AP. To keep the total traffic load in the network constant, we set the bitrate of the CBR traffic to 24 Mbps divided by the number of APs, where 24 Mbps is close to the effective transmission rate of 11g with 54 Mbps as the physical transmission rate.

## 5.2 Results

Figure 12 plots throughput versus  $n$  in topology I. The total throughput was high in the range of  $n \leq 4$ , while it decreased as  $n$  increased when  $n \geq 5$ . This is because as  $n$  increases, channel contention and frame collision occur more easily, which results in decreased throughput. The average throughput degraded drastically in the figure as  $n$  increased. According to the error bars, the difference between the maximum and minimum throughputs was small when  $n \leq 3$  and increased when  $n \geq 4$ . The minimum throughput was zero when  $n \geq 7$ , which indicates that some APs could not upload their data to the BS. Since the maximum number of hopcounts from APs to the BS increases as  $n$  increases, it is more difficult for APs further from the BS to deliver their data to their destination (the BS). This suggests that, in practice, we should operate our system in the range of  $n \leq 6$ . To operate the network in the range of  $n \geq 7$ , we should limit the uploading rates from APs so that APs far from the BS can deliver their data to the BS.

Figure 13 (a) plots throughput versus  $n$  in topology II. Note that in topology II, the number of APs  $N$  is equal to  $n^2$ . High total throughput was available when  $n \leq 3$ , while it degraded as  $n$  increased when  $n \geq 4$ . This is because as  $n$  becomes large, the network becomes more congested.

To focus on the throughput performance in the case of large numbers of APs, we show the average/minimum/maximum throughputs in the range of  $5 \leq n \leq 10$  in Figure 13 (b). The average throughput was smaller than 1 Mbps. According to the error bars, the differences in throughput among APs were large when  $n \geq 5$ . In particular, when  $n \geq 6$ , the minimum throughput was zero, which indicates that some APs could not upload data

Table 4: Simulation parameters for throughput evaluation

Parameter	Value
Wireless standard	IEEE802.11g
No. of channels	1
Frequency	2.4[GHz]
Physical transmission rate	54[Mbps]
Pathloss model	Two-ray
Routing protocol	AODV
Rate of CBR	24Mbps / no. of APs

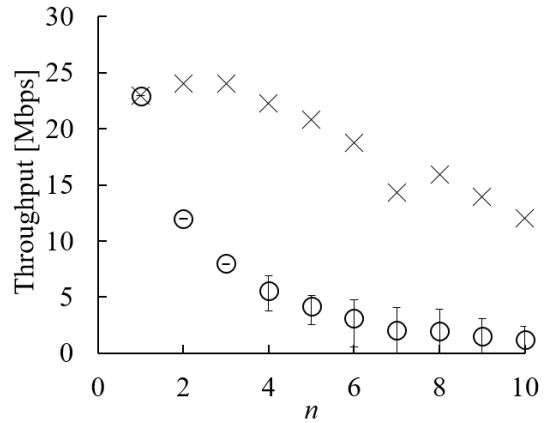


Figure 12: Throughput performance in topology I. Total throughput, average throughput, and maximum/minimum throughputs are plotted using  $\times$ s, circles, and error bars, respectively.

to the BS. Thus, in topology II, in practice, we should operate our system in the range of  $n \leq 5$ . As we mentioned for Figure 12, to operate the network in the range of  $n \geq 5$ , we should limit the uploading rates from APs so that APs far from the BS can deliver their sensor data to the BS.

## 6 Conclusions

This paper proposed a new design of wireless mesh networks formed by UAVs under the assumption that batteries and APs are replaceable and separable from UAVs and both are carried and placed at appropriate positions by the mechanical automation of UAVs. We first presented possible models of UAV-formed multihop networks and compared them. Then, we presented the problem formulation and the scheduling algorithm of UAVs. Through computer simulations, we numerically evaluated the number of UAVs that each model requires for maintaining a wireless mesh network. The simulation results suggested that the number of required UAVs is affected by the number of AP positions and can be minimized by introducing a battery replacement function. We also considered a realistic battery model and the required number of batteries and showed that our system performs well. Furthermore, throughput analysis demonstrated how our system performs as a wireless mesh-network infrastructure for sensor nodes. Future work will include implementation and experimental evaluation of the proposed system.

## Acknowledgement

This work was partly supported by JSPS KAKENHI Grant No. JP25730057 and No. 17H01732.

The authors would like to thank Mr. Yuki Goto, who graduated from Kyoto University in March 2017, and Ms. Miwa Tobita, who is currently a student of Kyoto University, for their suggestions.

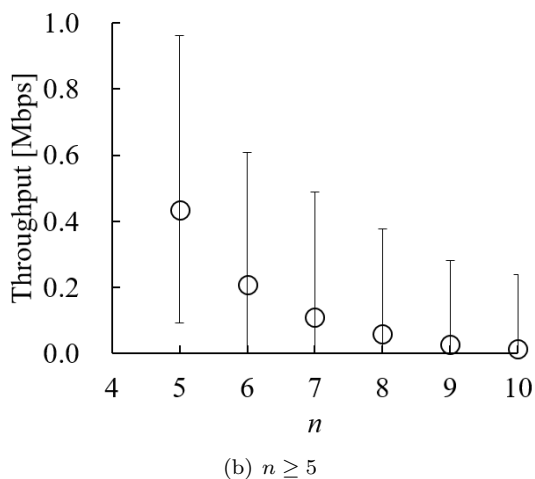
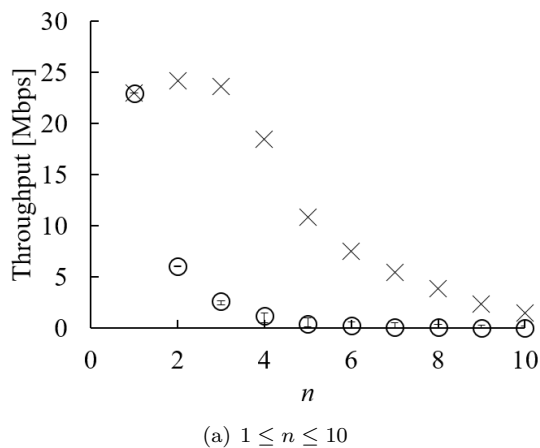


Figure 13: Throughput performance in topology II. Total throughput, average throughput, and maximum/minimum throughputs are plotted using  $\times$ s, circles, and error bars, respectively.

## References

- [1] I. Bekmezci, O. K. Sahingoz, and S. Temel, "Flying Ad-Hoc Networks (FANET): A Survey," *Ad Hoc Networks*, vol. 11, issue 3, pp. 1254-1270, May 2013.
- [2] T. Andre, K. Hummel, A. Schoellig, E. Yanmaz, M. Asadpour, C. Bettstetter, P. Grippa, H. Hellwagner, S. Sand, and S. Zhang, "Application-driven design of aerial communication networks," *IEEE Commun. Mag.*, vol. 52, no. 5, pp. 129-137, May 2014.
- [3] M. Erdelj and N. Enrico, "UAV-assisted disaster management: Applications and open issues," in *International Conference on Computing, Networking and Communications (ICNC)*, 2016, pp. 1-5.
- [4] A. Ahmed, M. Nagai, C. Tianen, and R. Shibasaki, "UAV based monitoring system and object detection technique development for a disaster area," *The International Archives of the Photogrammetry Remote Sensing and Spatial Information Sciences*, vol. 37, pp. 373-377, 2008.
- [5] G. Saggiani, F. Persiani, A. Ceruti, P. Tortora, E. Troiani, F. Giuletti, et al., "A UAV system for observing volcanoes and natural hazards," in *American Geophysical Union Fall Meeting*, 2007, vol. 1, p. 5.
- [6] M. Abdelkader, M. Shaqura, C. G. Claudel, and W. Gueaieb, "A uav based system for real time flash flood monitoring in desert environments using lagrangian microsensors," *Unmanned Aircraft Systems (ICUAS) 2013 International Conference*, 2013, pp. 25-34.
- [7] M. Di Felice, A. Trotta, L. Bedogni, K. R. Chowdhury, and L. Bononi, "Self-organizing aerial mesh networks for emergency communication," *IEEE 25th Annual International Symposium on Personal, Indoor, and Mobile Radio Communication (PIMRC)*, 2014, pp. 1631-1636.
- [8] K. Daniel, B. Dusza, A. Lewandowski, and C. Wietfeld, "AirShield: A system-of-systems MUAV remote sensing architecture for disaster response," in *IEEE Systems Conference (SysCon '09)*, 2009, pp. 196-200.
- [9] M. Quaritsch, K. Kruggl, D. Wischounig-Strucl, S. Bhattacharya, M. Shah, and B. Rinner, "Networked uavs as aerial sensor network for disaster management applications," *Elektrotechnik & Information-technik*, vol. 127, issue. 3, pp. 56-63, Mar 2010.
- [10] Q. Feng, J. McGeehan, and A. Nix, "Enhancing coverage and reducing power consumption in peer-to-peer networks through airborne relaying," in *65th IEEE Veh. Technol. Conf. (VTC)*, 2007, pp. 954-958.
- [11] S. Morgenthaler, T. Braun, Z. Zhao, T. Staub, and M. Anwender, "UAVNet: A mobile wireless mesh network using unmanned aerial vehicles," in *IEEE GLOBE-COM Wksp-WiUAV*, 2012, pp. 1603-1608.
- [12] K. Suzuki and J. Morrison, "Automatic battery replacement system for UAVs: Analysis and design," *Journal of Intelligent & Robotic Systems*, vol. 65, pp. 563-586, Jan 2012.
- [13] K. Swieringa, C. Hanson, J. Richardson, J. White, Z. Hasan, E. Qian, and A. Girard, "Autonomous battery swapping system for small-scale helicopters," in *IEEE International Conference on Robotics and Automation (ICRA)*, 2010, pp. 3335-3340.
- [14] F. P. Kemper, K. A. Suzuki, and J. R. Morrison, "UAV consumable replenishment: design concepts for automated service stations," *Journal of Intelligent & Robotic Systems*, vol. 61 issue 1, 369-397, Jan 2011.
- [15] T. Toksoz, J. Redding, M. Michini, B. Michini, J. P. How, M. Vavrina, and J. Vian, "Automated battery swap and recharge to enable persistent UAV missions," in *AIAA Infotech@Aerospace Conference*, 2011.
- [16] N. K. Ure, G. Chowdhary, T. Toksoz, J. P. How, M. A. Vavrina, and J. Vian, "An automated battery management system to enable persistent missions with multiple aerial vehicles," *IEEE/ASME Transactions on Mechatronics*, vol. 20, issue 1, pp. 275-286, Jan 2014.

- [17] K. Fujii, K. Higuchi, and J. Rekimoto, "Endless flyer: a continuous flying drone with automatic battery replacement," in IEEE 10th International Conference on Ubiquitous Intelligence and Computing and 10th International Conference on Autonomic and Trusted Computing (UIC/ATC), 2013, pp. 216-223.
- [18] P. E. Pounds and A. M. Dollar, "UAV rotorcraft in compliant contact: Stability analysis and simulation," in IEEE/RSJ International Conference on Intelligent Robots and Systems (IROS), 2011, pp. 2660-2667.
- [19] I. Palunko, P. Cruz, and R. Fierro, "Agile load transportation: Safe and efficient load manipulation with aerial robots," IEEE Robotics & Automation Magazine, vol. 19, issue 3, pp. 69-79, Sep 2012.
- [20] T. Bartelds, A. Capra, S. Hamaza, S. Stramigioli, and M. Fumagalli. "Compliant aerial manipulators: Toward a new generation of aerial robotic workers," IEEE Robotics and Automation Letters, vol. 1 issue 1, pp. 477-483, Jan 2016.
- [21] IEEE Technical Committee, Aerial Robotics and Unmanned Aerial Vehicles. [Online]. Available: <http://ieee-aerialrobotics-uavs.org/aerial-robots-uavs/aerial-manipulation/>
- [22] R. Shinkuma and Y. Goto, "Wireless multihop networks formed by unmanned aerial vehicles with separable access points and replaceable batteries," IEEE Ubiquitous Computing, Electronics & Mobile Communication Conference (UEMCON), pp.1-6, Oct 2016.
- [23] M. L. Cummings, S. Bruni, S. Mercier, and P. J. Mitchell, "Automation architecture for single operator, multiple UAV command and control," The International C2 Journal, vol. 1, no. 2, pp. 1-24, 2017
- [24] J. Kim, B. D. Song, and J. R. Morrison, "On the scheduling of systems of UAVs and fuel service stations for long-term mission fulfillment," Journal of Intelligent & Robotic Systems, Vol. 70, Issues 1-4, pp. 347-359 April 2013.
- [25] S. Tozlu, M. Senel, W. Mao, and A. Keshavarzian, "Wi-Fi enabled sensors for internet of things: A practical approach," IEEE Commun. Mag., vol. 50, issue 6, pp. 134-143, June 2012.
- [26] A. Ollero and L. Merino, "Unmanned aerial vehicles as tools for forest-fire fighting," Forest Ecology and Management, vol. 234, no. 1, p. 263, 2006.
- [27] L.W. Traub, "Calculation of Constant Power Lithium Battery Discharge Curves," Batteries 2.2, June 2016.
- [28] Parrot BEBOP2. [Online]. Available: <http://global.parrot.com/products/bebop2/>
- [29] Lithium Ion UPF614496. [Online]. Available: [http://www.panamar.it/images/date\\_sheets\\_UPF-614496.pdf](http://www.panamar.it/images/date_sheets_UPF-614496.pdf)
- [30] QualNet Network Simulator.[Online]. Available: <http://web.scalable-networks.com/qualnet-network-simulator>
- [31] J. Li, Y. Fan, H. Chen, K. Xu, Y. Dai, F. Yin, and Y. Ji, "Radio-over-fiber-based distributed antenna systems supporting IEEE 802.11 N/AC standards," in IEEE 12th International Conference on Optical Communications and Networks (ICOCN), 2013.
- [32] V.K. Jones and H. Sampath, "Emerging technologies for WLAN," IEEE Commun. Mag., vol. 53, issue 3, pp. 141-149, Mar 2015.
- [33] C. Perkins, E. Belding-Royer, and S. Das, "Ad hoc on-demand distance vector (AODV) routing," RFC 3561, 2003.



**Ryoichi Shinkuma** received the B.E., M.E., and Ph.D. degrees in Communications Engineering from Osaka University, Japan, in 2000, 2001, and 2003, respectively. In 2003, he joined the faculty of Communications and Computer Engineering, Graduate School of Informatics, Kyoto University, Japan, where he is currently an Associate Professor. He was a Visiting Scholar at Wireless Information Network Laboratory (WINLAB), Rutgers, the State University of New Jersey, USA, from 2008 Fall to 2009 Fall. His research interests include network design and control criteria, particularly inspired by economic and social aspects. He received the Young Researchers' Award from IEICE in 2006 and the Young Scientist Award from Ericsson Japan in 2007, respectively. He also received the TELECOM System Technology Award from the Telecommunications Advancement Foundation in 2016. He has been the chairperson of the Mobile Network and Applications (MoNA) Technical Committee of IEICE Communications Society since June 2017. He is a member of IEEE.



**Narayan B. Mandayam** (S'89-M'94-SM'99-F'09) received the B.Tech (Hons.) degree in 1989 from the Indian Institute of Technology, Kharagpur, and the M.S. and Ph.D. degrees in 1991 and 1994 from Rice University, all in electrical engineering. Since 1994 he has been at Rutgers University where he is currently a Distinguished Professor and Chair of the Electrical and Computer Engineering department. He also serves as Associate Director at WINLAB. He was a visiting faculty fellow in the Department of Electrical Engineering, Princeton University, in 2002 and a visiting faculty at the Indian Institute of Science, Bangalore, India in 2003. Using constructs from game theory, communications and networking, his work has focused on system modeling, information processing and resource management for enabling cognitive wireless technologies to

support various applications. He has been working recently on the use of prospect theory in understanding the psychophysics of pricing for wireless data networks as well as the smart grid. His recent interests also include privacy in IoT, resilient smart cities as well as modeling and analysis of trustworthy knowledge creation on the internet. Dr. Mandayam is a co-recipient of the 2015 IEEE Communications Society Advances in Communications Award for his seminal work on power control and pricing, the 2014 IEEE Donald G. Fink Award for his IEEE Proceedings paper titled "Frontiers of Wireless and Mobile Communications" and the 2009 Fred W. Ellersick Prize from the IEEE Communications Society for his work on dynamic spectrum access models and spectrum policy. He is also a recipient of the Peter D. Cherasia Faculty Scholar Award from Rutgers University (2010), the National Science Foundation CAREER Award (1998) and the Institute Silver Medal from the Indian Institute of Technology (1989). He is a coauthor of the books: Principles of Cognitive Radio (Cambridge University Press, 2012) and Wireless Networks: Multiuser Detection in Cross-Layer Design (Springer, 2004). He has served as an Editor for the journals IEEE Communication Letters and IEEE Transactions on Wireless Communications. He has also served as a guest editor of the IEEE JSAC Special Issues on Adaptive, Spectrum Agile and Cognitive Radio Networks (2007) and Game Theory in Communication Systems (2008). He is a Fellow and Distinguished Lecturer of the IEEE.